

## Structure of the Interface between Two Polar Liquids: Nitrobenzene and Water

Guangming Luo,<sup>†</sup> Sarka Malkova,<sup>†</sup> Sai Venkatesh Pingali,<sup>†</sup> David G. Schultz,<sup>†,‡</sup> Binhua Lin,<sup>§</sup> Mati Meron,<sup>§</sup> Ilan Benjamin,<sup>\*,||</sup> Petr Vanysek,<sup>\*,⊥</sup> and Mark L. Schlossman<sup>\*,†,‡</sup>

Department of Physics, Department of Chemistry, University of Illinois at Chicago, Chicago, Illinois 60607, The Center for Advanced Radiation Sources, University of Chicago, Chicago, Illinois 60637, Department of Chemistry, University of California, Santa Cruz, California, 95064, and Department of Chemistry and Biochemistry, Northern Illinois University, DeKalb, Illinois 60115

Received: December 6, 2005; In Final Form: January 17, 2006

Synchrotron X-ray reflectivity is used to study the electron density as a function of depth through the bulk nitrobenzene–water interface at four different temperatures. The measured interfacial width differs from the predictions of capillary wave theory with a progressively smaller deviation as the temperature is raised. Computer simulations suggest the presence of both molecular layering and dipole ordering parallel to the interface. Either layering or a bending rigidity, that can result from dipole ordering, can explain these measurements.

## Introduction

Numerous electron and ion transfer processes important in chemical and biological systems occur at interfaces between phases of soft matter such as that between two liquids.<sup>1</sup> Fundamental questions remain about these processes, partially because the structure of the liquid–liquid interface is not well understood. Recent X-ray scattering studies of the interface between nonpolar alkane oils and water revealed contributions to the interfacial width from both molecular ordering of the alkane and interfacial roughness due to thermal capillary waves.<sup>2</sup> However, the solubility of electrolytes in nonpolar oils is very low and the use of these oils for charge-transfer processes is limited. Less is known about the structure of the interface between a polar oil and water, despite the many examples of electron and ion transfer at these interfaces.<sup>1</sup> It has been proposed that solvent mixing occurs at the polar oil/water interface and is important for these transfer processes (see references in ref 3). However, the results presented here and earlier results on the water/2-heptanone interface are consistent with molecular dynamics simulations that predict a locally sharp but rough interface without solvent mixing.<sup>3,4</sup> In addition, the structure of these interfaces is affected by the presence of dipolar molecules in both phases and their dipole interactions across the interface. These interactions can order the molecules, either orientationally or spatially, thereby altering the elastic properties of the interface, such as its bending rigidity.

The interface between nitrobenzene (dielectric constant  $\epsilon = 34.8$  at 25 °C) and water ( $\epsilon = 78.85$  at 25 °C) is commonly used as a model system to study interfacial electron and ion

transport.<sup>5</sup> We show that the X-ray reflectivity from this interface at four different temperatures is larger than that predicted by the capillary wave theory of Buff, Lovett, and Stillinger (BLS).<sup>6</sup> This excess reflectivity can be explained by either an interfacial bending rigidity (i.e., an energy cost due to bending a constant area interface) or by layering of nitrobenzene molecules near the interface. These effects may not be independent and it can be expected that layering will generate a bending rigidity. However, since our experiments do not have the resolution to separate these two effects, we provide an analysis that considers separately the influence of layering and bending rigidity.

## Data and Analysis

X-ray reflectivity was measured at the ChemMatCARS beamline 15-ID at the Advanced Photon Source (Argonne National Laboratory) with a liquid surface spectrometer and measurement techniques described in detail elsewhere.<sup>7,8</sup> For specular reflection, which probes the electron density as a function of depth through the interface, the wave vector transfer is in the  $z$ -direction, normal to the interface;  $Q_z = (4\pi/\lambda) \sin \alpha$ , where  $\lambda = 0.41360 \pm 0.00005$  Å is the X-ray wavelength for these measurements,  $\alpha$  is the angle of reflection, and  $Q_x = Q_y = 0$  (in the plane of the interface). Purified water (Milli-Q) and nitrobenzene (Fluka puriss.  $\geq 99.5\%$  filtered through basic alumina) were contained in a vapor-tight, Mylar-lined, stainless steel sample cell with Mylar X-ray windows.

Figure 1 illustrates the X-ray reflectivity,  $R(Q_z)$ , measured from the nitrobenzene–water interface at four temperatures.<sup>9</sup> The interfacial width  $\sigma$  is determined by fitting these data to<sup>10</sup>

$$R(Q_z) \approx \left| \frac{Q_z - Q_z^T}{Q_z + Q_z^T} \right|^2 \exp(-Q_z Q_z^T \sigma^2) \quad (1)$$

where  $Q_z^T = \sqrt{Q_z^2 - Q_c^2}$  is the  $z$ -component of wave vector

\* To whom correspondence should be addressed, E-mail: schloss@uic.edu, pvanysek@niu.edu, benjamin@chemistry.ucsc.edu.

<sup>†</sup> Department of Physics, University of Illinois at Chicago.

<sup>‡</sup> Department of Chemistry, University of Illinois at Chicago.

<sup>§</sup> The Center for Advanced Radiation Sources, University of Chicago.

<sup>||</sup> Department of Chemistry, University of California.

<sup>⊥</sup> Chemistry and Biochemistry, Northern Illinois University.

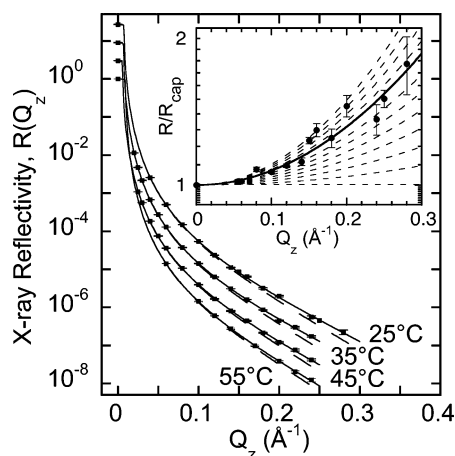


**Figure 1.** X-ray reflectivity from the nitrobenzene–water interface at four temperatures. Solid lines are fits to eq 1. Dashed lines are calculated using  $\sigma_{\text{cap}}$  (eq 2) in eq 1. Data at different temperatures are offset by factors of 3 ( $R = 1$  at  $Q_z = 0$ ). Inset: The inset shows the 25 °C data and calculated reflectivities on a log scale (for different values of interfacial width) normalized to the reflectivity ( $R_{\text{cap}}$ ) calculated for the width  $\sigma_{\text{cap}} = 5.2$  Å. The calculated reflectivities in the inset are given by the lines (dashed and solid) for widths  $\sigma = 4.1$  Å to  $5.2$  Å in steps of  $0.1$  Å (top to bottom). The solid line is the best fit value  $\sigma = 4.5$  Å. The same series of lines in the inset can be calculated by adjusting  $\kappa$  in eq 3 so  $\sigma_H$  takes on the values  $4.1$  Å to  $5.2$  Å. This yields values of  $\kappa = 80, 40, 22, 11, 6, 3, 1.29, 0.6, 0.25, 0.11, 0.04$ , and  $0$   $k_B T$  from top to bottom.

transfer with respect to the lower phase and  $Q_c \approx 4\sqrt{\Delta\rho r_c \pi}$  is the critical value of  $Q_z$  for total reflection ( $\Delta\rho = \rho_w - \rho_n$ , e.g., at 25 °C,  $\rho_w = 0.3333$  e $^-/\text{\AA}^3$  for pure water and  $\rho_n = 0.3766$  e $^-/\text{\AA}^3$  for pure nitrobenzene,<sup>11</sup>  $r_c \approx 2.818$  fm). The solid lines shown in Figure 1 are fits to eq 1 using two fitting parameters,  $\sigma$  and  $Q_{\text{offset}}$ , and calculated values of  $Q_c$  (where  $Q_z$  in eq 1 is replaced by  $Q_z - Q_{\text{offset}}$ ).<sup>11</sup>  $Q_{\text{offset}}$  ( $\leq 10^{-3}$  Å $^{-1}$ ) represents a typical accuracy for instrumental alignment. Additional fits (not shown) that include  $Q_c$  as a fitting parameter yield values of  $Q_c$  within  $10^{-4}$  Å $^{-1}$  of the calculated values.

The dashed lines in Figure 1 are calculated from eq 1 using values of the interfacial width  $\sigma_{\text{cap}}$  calculated from the BLS capillary wave theory,<sup>6,12</sup>

$$\sigma_{\text{cap}}^2 = \frac{k_B T}{2\pi} \int_{q_{\min}}^{q_{\max}} \frac{q dq}{\gamma q^2 + \Delta\rho_m g} \approx \frac{k_B T}{2\pi\gamma} \log\left(\frac{q_{\max}}{q_{\min}}\right) \quad (2)$$

where  $k_B T$  is the Boltzmann constant times the temperature,  $\gamma$  is the interfacial tension measured with a Teflon Wilhelmy plate (in agreement with literature values<sup>13</sup>),  $\Delta\rho_m$  is the mass density difference of the two phases,  $g$  is the gravitational acceleration,  $q_{\min} = (2\pi/\lambda) \Delta\beta \sin\alpha$  (with the angular acceptance of the detector  $\Delta\beta = 4.7 \times 10^{-4}$  rad),<sup>2</sup> and  $\Delta\rho_m g \ll \gamma q_{\min}^2$ . The variable  $q$  is the in-plane wave vector of the capillary waves. The limit,  $q_{\max}$ , is determined by the cutoff for the smallest wavelength capillary waves that the interface can support. We have chosen  $q_{\max} = 2\pi/5$  Å $^{-1}$  where  $5$  Å is an approximate molecular size. Note that  $\sigma_{\text{cap}}$  depends on  $q_{\max}$  logarithmically and is not very sensitive to its value.

The dashed lines in Figure 1 lie below the measured data because the calculated values of  $\sigma_{\text{cap}}$  are larger than the measured  $\sigma$  (Table 1). The inset to Figure 1 illustrates the ratio of the data at  $T = 25$  °C to the reflectivity calculated for the width  $\sigma_{\text{cap}} = 5.2$  Å. The inset also shows the ratio of calculated reflectivities for other interfacial widths to the  $\sigma = 5.2$  Å reflectivity. The variation of the data and its best fit from the

**TABLE 1: Properties of Nitrobenzene–Water Interfaces<sup>a</sup>**

temperature (°C) ( $\pm 0.03$ )	interfacial tension $\gamma$ ( $10^{-3}$ N/m) ( $\pm 0.2$ )	$\sigma_{\text{measured}}$ (Å) ( $\pm 0.1$ )	$\sigma_{\text{cap}}$ (Å) ( $\pm 0.02$ )	$\kappa$ ( $k_B T$ )
25.00	25.2	4.5	5.17	6
35.00	24.5	4.5	5.24	6
45.00	23.8	4.8	5.42	3
55.00	22.9	5.1	5.62	1

<sup>a</sup>  $\sigma_{\text{measured}}$  is the measured interfacial width.  $\sigma_{\text{cap}}$  is calculated from eq 2.  $\kappa$  is the bending rigidity calculated from eq 3 that yields  $\sigma_H = \sigma_{\text{measured}}$ . The accuracy of  $\kappa$  can be judged from the inset in Figure 1.

straight line at  $R/R_{\text{cap}} = 1$  shows that the measured width  $\sigma$  is smaller than the calculated values of  $\sigma_{\text{cap}}$  by several standard deviations (see also Table 1).

The calculated value of  $\sigma_{\text{cap}}$  can be brought into agreement with the measured width if  $q_{\max}$  is chosen to be  $\sim 2\pi/50$  Å $^{-1}$ , but there is no physical reason to expect that the smallest wavelength capillary wave is  $50$  Å, much larger than any relevant length scale. An explanation for the smaller measured width is that the capillary waves are damped by an interfacial bending rigidity. In this case, distortions of the interface require an additional energy as described by the Helfrich Hamiltonian.<sup>14</sup> Equation 2 is then generalized to<sup>15</sup>

$$\sigma_H^2 = \frac{k_B T}{2\pi} \int \frac{q dq}{\gamma q^2 + \kappa q^4 + \Delta\rho_m g} \approx \frac{k_B T}{2\pi\gamma} \ln \frac{(\gamma/\kappa)^{1/2}}{q_{\min}} \quad (3)$$

where  $\kappa$  is the bending rigidity. Since the  $\kappa$  term is proportional to  $q^4$ , whereas the  $\gamma$  term is proportional to  $q^2$ , the effect of  $\kappa$  is to damp the smaller wavelength, i.e., larger  $q$ , fluctuations. Values of  $\kappa$  that yield values of  $\sigma_H$  in agreement with our measured values of  $\sigma$  are listed in Table 1. Note that the quantity  $\sigma$  is fit to the data, not  $\kappa$ , and that error bars on  $\kappa$  (not stated) have a nonlinear relationship with  $\sigma$ . An example of this is the  $\kappa$  values given in the Figure 1 caption that would produce the calculated  $\sigma$  values used in the inset to Figure 1.

Previous reflectivity measurements of the interface between water and nonpolar alkane liquids have not provided evidence for a bending rigidity,<sup>2</sup> though other types of measurements on pure liquid surfaces and on interfaces with surfactants and internal interfaces in surfactant solutions have determined bending rigidities on the order of one to tens of  $k_B T$ .<sup>16–18</sup> For an interface between two dipolar liquids, it is plausible that the interfacial distortion of orientationally ordered molecules on both sides of the interface can lead to a bending rigidity. A molecular dynamics simulation of the nitrobenzene–water interface at 25 °C demonstrated that interfacial nitrobenzene and water dipoles are preferentially aligned parallel to the interface.<sup>3</sup> Extension of this earlier molecular dynamics simulation<sup>3</sup> using the same intermolecular potentials and methodology but run for a longer time (4 ns, as compared to 1.5 ns) and for an additional temperature, 55 °C, indicates that the preferential alignment is reduced by  $\sim 30\%$  at the higher temperature (Figure 2). If dipole ordering is the cause of a bending rigidity, then the more isotropic orientational distribution at 55 °C is qualitatively consistent with a lower bending rigidity at higher temperatures.

Figure 3 illustrates the interfacial electron density profiles determined from the molecular dynamics simulations. A previously published simulation<sup>3</sup> was not fully equilibrated and exhibited larger amplitude peaks on the nitrobenzene side. The simulation shown in Figure 3 produced an essentially unchanged profile after  $\sim 2$  ns. The profiles exhibit rapidly damped layering of the disk-shaped nitrobenzene molecules with a layer spacing of  $\sim 8$  Å. The layer amplitudes are smaller at higher temperature.

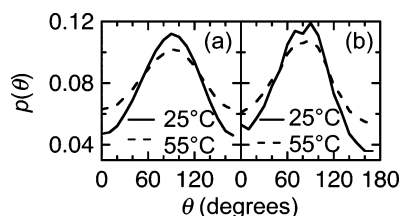


**Figure 2.** (a) Water dipole and (b) nitrobenzene dipole orientational distribution at the nitrobenzene–water interface determined by molecular dynamics simulation. Each distribution is calculated using a 6 Å wide slab centered at the Gibbs dividing surface. The distributions are normalized such that  $\int_0^\pi \rho(\theta) \sin \theta d\theta = 1$ , where  $\theta$  is the angle between the dipole and the normal to the interface. The distributions show that the dipoles tend to lie parallel to the interface.

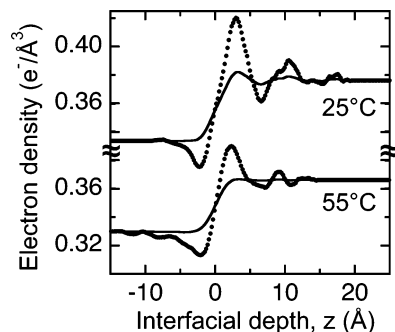


**Figure 3.** Dots, electron density profile from molecular dynamics (MD) simulation. Solid line, MD simulation scaled by an amplitude as discussed in text.<sup>20</sup> Although the scaling factor for the two temperatures is nearly the same ( $\sim 0.18$ ), the scaled 55 °C profile appears to have much lower amplitude oscillations because of the overlap with the error function representing the interfacial capillary waves.  $z > 0$  is nitrobenzene;  $z < 0$  is water.

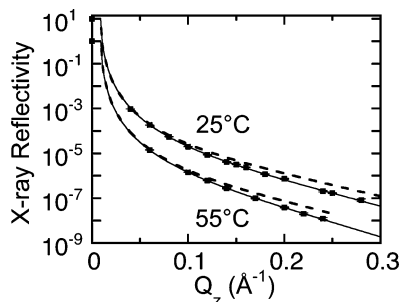


**Figure 4.** X-ray reflectivity,  $R(Q_z)$ . Dots, data as in Figure 1; solid lines, fits to model oscillation profiles; dashed lines, reflectivity predicted from MD profiles convoluted with a Gaussian. Data at 25 °C and 55 °C offset by a factor of 10.

Calculations of the X-ray reflectivity from the Parratt algorithm<sup>19</sup> for interfaces with these electron density profiles yield values much larger than the experimental measurements (not shown). This is due primarily to the small cross section of the simulation cell (3.13 nm),<sup>2</sup> that restricts the range of capillary wave vectors to being much smaller than that probed by experiment. The effect of capillary waves with wave vectors corresponding to the size of the molecular dynamics simulation cell,  $2\pi/31.3 \text{ Å}^{-1}$ , down to the experimental value of  $q_{\min}$  can be included by using eq 2 to calculate an interfacial width that will be referred to as  $\sigma_{\text{gauss}}$  ( $= 4.57 \text{ Å}$  at 25 °C, and  $5.08 \text{ Å}$  at 55 °C), then convoluting the electron density profile with  $(1/\sigma_{\text{gauss}} \sqrt{2\pi}) \exp(-z^2/2\sigma_{\text{gauss}}^2)$ . As shown in Figure 4, the reflectivity calculated from this modified simulation is still larger than the measured reflectivity.

Although the MD simulations do not provide a definitive explanation for our measurements, they suggest that nitroben-

zene layering is relevant. To test this idea, we used the form of the electron density from the simulation, but adjusted the amplitude of the oscillations with a single fitting parameter to fit our data.<sup>20</sup> Figure 3 illustrates the model oscillation profiles that fit the data. The best fit profiles require the oscillations in the simulation profiles to be scaled by a factor of 0.19 for the 25 °C sample and by a factor of 0.17 for the 55 °C sample. Capillary wave roughening is added to this model by convoluting the electron density profiles with a Gaussian of width  $\sigma_{\text{gauss}}$ . Figure 4 illustrates that this model provides a fit of equivalent quality to the fit in Figure 1 based upon the bending rigidity model of eq 3.

## Discussion

Although our measurements are consistent with the layering of nitrobenzene at the interface, these measurements do not have adequate resolution to explore the detailed structure of the layering profile or to definitively distinguish the effects of layering from those of a bending rigidity. It is instructive to compare these measurements to observations of atomic layering at the liquid–vapor interface of liquid metals.<sup>21</sup> The small surface roughness ( $< 1 \text{ Å}$ ) of liquid metals and the negligible scattering from the vapor allows for the measurement of a peak in the reflectivity, at high  $Q_z$ , that is a signature of the atomic layering. The larger interfacial roughness of the nitrobenzene–water interface reduces the amplitude of a layering peak and, in addition, reduces the reflectivity far below the measurable level at the  $Q_z$  anticipated for that peak ( $\sim 0.8 \text{ Å}^{-1}$ ). Off-specular diffuse scattering is another technique that could provide complementary information on the interfacial roughness and rigidity, but the background scattering in this experimental geometry precludes its measurement.

Mecke and Dietrich recently introduced a density functional theory of the liquid–vapor interface of hard spheres interacting via isotropic van der Waals forces that reconciles the van der Waals description of an intrinsic interface with the BLS approach to capillary waves.<sup>22</sup> This theory, and a variation of it, has been used to describe the liquid–vapor interface of water, several organic liquids, and liquid gallium.<sup>18,23,24</sup> Applied to our experiment, it yields unreasonably large values of the parameter  $C_H$ .<sup>25</sup> Greater bending energies can be expected for an intrinsic interface of layered dipoles interacting via an anisotropic dipole force as compared to hard spheres interacting via van der Waals forces as in the Mecke–Dietrich theory.

In summary, X-ray reflectivity was used to probe the structure of an interface between two polar liquids. These results are consistent with an interface that is locally sharp on the molecular scale, in agreement with MD simulations but in contrast with some recent theories of this interface used to describe transfer processes.<sup>26–28</sup> A structure determined solely by the macroscopic interfacial tension cannot describe our results. It is necessary to consider the existence of either interfacial layering or an interfacial bending rigidity to explain our measurements. It is anticipated that distortions of a layered profile by short wavelength interfacial oscillations will generate a bending rigidity.<sup>22</sup> Significant advances in experimental design will be needed to distinguish between these two effects at this interface.

**Acknowledgment.** M.L.S. and P.V. acknowledge support from NSF–CHE0315691, I.B. from NSF–CHE0345361. M.L.S. acknowledges Moshe Deutsch for a discussion on interfacial layering. ChemMatCARS is supported by NSF–CHE, NSF–DMR, and the DOE. The APS is supported by the DOE Office of Basic Energy Sciences.

## References and Notes

- (1) Volkov, A. G. *Liquid Interfaces in Chemical, Biological, and Pharmaceutical Applications*; Marcel Dekker: New York, 2001.
- (2) Mitrinovic, D. M.; Tikhonov, A. M.; Li, M.; Huang, Z.; Schlossman, M. L. *Phys. Rev. Lett.* **2000**, *85*, 582.
- (3) Michael, D.; Benjamin, I. *J. Electroanal. Chem.* **1998**, *450*, 335.
- (4) Luo, G.; Malkova, S.; Pingali, S. V.; Schultz, D. G.; Lin, B.; Meron, M.; Graber, T.; Gebhardt, J.; Vanysek, P.; Schlossman, M. L. *Electrochem. Commun.* **2005**, *7*, 627.
- (5) Vanysek, P. *Electrochemistry on Liquid/Liquid Interfaces*; Springer-Verlag: Berlin, 1985.
- (6) Buff, F. P.; Lovett, R. A.; Stillinger, F. H. *Phys. Rev. Lett.* **1965**, *15*, 621.
- (7) Schlossman, M. L.; Synal, D.; Guan, Y.; Meron, M.; Shea-McCarthy, G.; Huang, Z.; Acero, A.; Williams, S. M.; Rice, S. A.; Viccaro, P. J. *Rev. Sci. Instrum.* **1997**, *68*, 4372.
- (8) Zhang, Z.; Mitrinovic, D. M.; Williams, S. M.; Huang, Z.; Schlossman, M. L. *J. Chem. Phys.* **1999**, *110*, 7421.
- (9) Luo, G.; Malkova, S.; Pingali, S. V.; Schultz, D. G.; Schlossman, M. L.; Vanysek, P.; Lin, B.; Meron, M.; Graber, T.; Gebhardt, J. *Faraday Discuss.* **2005**, *129*, 23.
- (10) Nevot, L.; Croce, P. *Rev. Phys. Appl.* **1980**, *15*, 761.
- (11) Water densities from *Handbook of Chemistry and Physics*, 70th ed.; CRC Press: Boca Raton, FL 1989, pure nitrobenzene densities measured by a pycnometer: 1.203 g/mL at 25 °C, 1.192 g/mL at 35 °C, 1.180 g/mL at 45 °C, 1.170 g/mL at 55 °C; bulk solubilities from S. N. Pepelyayev, V. A. Shilnikov, and N. P. Uglev, *Russ. J. Appl. Chem.* **1990**, *63*, 1854.
- (12) Schwartz, D. K.; Schlossman, M. L.; Kawamoto, E. H.; Kellogg, G. J.; Pershan, P. S.; Ocko, B. M. *Phys. Rev. A* **1990**, *41*, 5687.
- (13) Reid, J. D.; Melroy, O. R.; Buck, R. P. *J. Electroanal. Chem.* **1983**, *147*, 71.
- (14) Helfrich, W. *Z. Naturforsch.* **1973**, *28c*, 693.
- (15) Zielinska, B. J. A.; Bedeaux, D.; Vlieger, J. *Physica A* **1981**, *107*, 91.
- (16) Servuss, R. M.; Harbich, W.; Helfrich, W. *Biochim. Biophys. Acta* **1976**, *436*, 900.
- (17) Schneider, M. B.; Jenkins, J. T.; Webb, W. W. *J. Phys. (Paris)* **1984**, *45*, 1457.
- (18) Mora, S.; Daillant, J.; Mecke, K.; Luzet, D.; Braslau, A.; Alba, M.; Struth, B. *Phys. Rev. Lett.* **2003**, *90*, 216101.
- (19) Parratt, L. G. *Phys. Rev.* **1954**, *95*, 359.
- (20) The scaling of the oscillations involved subtraction of a background density modeled by an error function profile whose width is given by capillary waves calculated for the simulations (2.18 Å), multiplication of the oscillations by a single, adjustable amplitude, and recombination of the oscillations with the error function profile. Although deconvolution and reconvolution would rigorously remove and add back the capillary waves, the simulation data did not allow this to be done accurately.
- (21) Magnussen, O. M.; Ocko, B. M.; Regan, M. J.; Penanen, K.; Pershan, P. S.; Deutsch, M. *Phys. Rev. Lett.* **1995**, *74*, 4444.
- (22) Mecke, K. R.; Dietrich, S. *Phys. Rev. E* **1999**, *59*, 6766.
- (23) Fradin, C.; Braslau, A.; Luzet, D.; Smilgies, D.; Alba, M.; Boudet, N.; Mecke, K.; Daillant, J. *Nature* **2000**, *403*, 871.
- (24) Li, D.; Yang, B.; Lin, B.; Meron, M.; Gebhardt, J.; Graber, T.; Rice, S. A. *Phys. Rev. Lett.* **2004**, *92*, 136102.
- (25) Using the product approximation (eq 3.60 in ref 22) along with a critical temperature of 240 °C, a value of  $C_H = 8$  is required to predict  $\sigma = 4.5$  Å that was measured at 25 °C (note, if  $C_H = 0.25$ , the value predicted from Landau theory, then  $\sigma = 6.6$  Å). This value of  $C_H$  is most likely unphysical because it yields values of  $\gamma$  at the smallest values of  $q$  ( $\approx 2\pi/5$  Å<sup>-1</sup>) that are 2 orders of magnitude larger than the macroscopic tension.
- (26) Henderson, D. J.; Schmickler, W. *J. Chem. Soc., Faraday Trans.* **1996**, *92*, 3839.
- (27) Pereira, C. M.; Schmickler, W.; Silva, A. F.; Sousa, M. J. *Chem. Phys. Lett.* **1997**, *268*, 13.
- (28) Frank, S.; Schmickler, W. *J. Electroanal. Chem.* **2000**, *483*, 18.